Follow us @BoneJointRes

Freely available online OPEN ACCESS

BJR

BIOMECHANICS

Thickness of simple calcaneal tuberosity avulsion fractures influences the optimal fixation method employed

C. Wang,
S-J. Liu,
C-H. Chang

From National Taiwan University Hospital, Taipei City, Taiwan

Aims

This study aimed to establish the optimal fixation methods for calcaneal tuberosity avulsion fractures with different fragment thicknesses in a porcine model.

Methods

A total of 36 porcine calcanea were sawed to create simple avulsion fractures with three different fragment thicknesses (5, 10, and 15 mm). They were randomly fixed with either two suture anchors or one headless screw. Load-to-failure and cyclic loading tension tests were performed for the biomechanical analysis.

Results

This biomechanical study predicts that headless screw fixation is a better option if fragment thickness is over 15 mm in terms of the comparable peak failure load to suture anchor fixation (headless screw: 432.55 N (SD 62.25); suture anchor: 446.58 N (SD 84.97)), and less fracture fragment displacement after cyclic loading (headless screw: 3.94 N (SD 1.76); suture anchor: 8.68 N (SD 1.84)). Given that the fragment thickness is less than 10 mm, suture anchor fixation is a safer option.

Conclusion

Fracture fragment thickness helps in making the decision of either using headless screw or suture anchor fixation in treating calcaneal tuberosity avulsion fracture, based on the regression models of our study.

Cite this article: *Bone Joint Res* 2023;12(8):504–511.

Keywords: Avulsion fracture, Pullout strength, Calcaneal tuberosity fracture, Headless screw, Suture anchor

Article focus

- How does the fragment thickness of an avulsion fracture affect the pullout strength of headless screw and suture anchor fixation?
- How do headless screw and suture anchor fixation behave when treating calcaneal avulsion fracture with various thicknesses in mechanical testing?
- Can headless screw fixation be an alternative for avulsion fracture fixation, and if so, when should it be used?

Key messages

- Fragment thickness affects the pullout strength of headless screw fixation more than suture anchor fixation.
- The pullout strength of headless screw fixation is comparable to suture anchor fixation when the fragment thickness is above 15 mm.
- Preoperative or intraoperative measurement of avulsed fragment thickness could help to decide the optimal fixation method to use.

Strengths and limitations

- For the first time, the current study investigates the effects of avulsed fragment thickness on fixation strength of headless screw and suture anchor in the calcaneal avulsion fracture.
- This study did not take osteoporotic porcine bones for testing models, which possibly affects its applicability to calcaneal tuberosity avulsion fractures.
- Further clinical studies should be conducted to validate the effects of the

Correspondence should be sent to Chung-Hsun Chang; email: jonathanchchang@gmail.com

doi: 10.1302/2046-3758.128.BJR-2023-0060.R1

Bone Joint Res 2023;12(8):504–511.

avulsed fragment thickness on headless screw and suture anchor fixation.

Introduction

A calcaneal tuberosity avulsion fracture is not an uncommon fracture, which usually affects women in their seventh decade.[1] The fracture fragments are usually 2 to 3 cm long and are situated in the posterosuperior portion of the posterior tuberosity,[2] where the Achilles tendon sits. Surgery is usually indicated for the displaced fracture. A plethora of surgical fixation methods have been described in the literature, such as tension banding wiring or cannulated screws combined with cerclage wires; however, poor bone qualities[3,4] and high risks of postoperative wound complications mean that there is currently no consensus on the best fixation methods.[5,6] The poor bone quality of this fracture makes complex suture fixation the most commonly applied surgical technique.[7-9] However, lag screw fixation is an alternative when the fracture fragment is sufficiently large.[10-12]

Screw pullout is one of the most common failure mechanisms of screw fixation.[13,14] Khazen et al[11] suggest that lag screws combined with suture anchors provide better fixation. Wheeler and McLoughlin[15] demonstrated that lag screw provides lower pullout strength than the all-threaded headless screw. The fully threaded design of the headless screw allows greater pullout strength, while its variable pitches lead to better compression, thus accelerating bone healing.[16,17] Additionally, screw fixation is relatively easily applied and thus decreases surgical time. Nevertheless, use of a headless screw for calcaneal avulsion or similar fractures is seldom discussed in the literature.

Since suture fixation is the most common strategy to deal with calcaneal tuberosity fracture, we decided to compare suture fixation with headless screw fixation. The fragment thickness is one of the determining factors for the pullout strength of a screw, and should be taken into consideration for fixation methods.[18] However, the optimal thickness of the fracture fragment for the screw fixation is not discussed much in the literature. To investigate the effect of fragment thickness on calcaneal tuberosity avulsion fracture, we decided to compare headless screw fixation to suture fixation with suture anchors only, to minimize the complexity of the fixation construct. This study aimed to provide surgeons with evidence of value-based treatment for decision-making. Therefore, we believe that this is the first study to compare headless screw and suture anchor fixation for simple calcaneal avulsion fracture with different thicknesses, and to determine the optimal fixation methods.

Methods

Biomechanical model. This study used one-year-old porcine heels (*Sus scrofa domestica*) stored at -20°C before shipping. The National Taiwan University Hospital Medicine Institution Animal Care and Use Committee exempted this study to apply for approval fulfilling ARRIVE criteria because of the direct use of animal explants from an abattoir. Before the experiment, the samples were thawed at 4°C for 24 hours. Bone mineral density (BMD) was measured by scanning the 2 cm central portion of each sample using micro-CT (Skyscan 1176; Bruker, USA).[19-21] After micro-CT, the 3D-printed cutting jig was applied to saw the calcaneal tuberosity to make an artificial fracture mimicking a calcaneal tuberosity avulsion fracture with the designated thickness of 5, 10, or 15 mm (12 heels in each thickness). The fractured fragment was further shaped into a cuboid with a 12 × 12 mm^2 area to standardize the fragment shape. The height, width, and length of every fracture fragment were measured using a calliper.

Study group. To investigate the effect of fracture fragment thickness in headless screw and suture anchor fixation, we created three groups with different fragment thicknesses (5, 10, and 15 mm) for both fixations. There were six subgroups in total, and each subgroup contained six porcine heels. In each subgroup, three heels were tested in the load-to-failure tests while the other three received cyclic loading tests.

Fixation technique. For headless screw fixation (Acutrak 2: 30 mm in length; Acumed, USA), the fragment was manually reduced, and a 1.2 mm Kirschner wire (K-wire) was used for temporary fixation and anti-rotation. The guidewire then passed through the tendon and was inserted perpendicularly to the fracture plane. A 30 mm standard-sized headless screw was inserted and tightened over the guidewire until the whole screw was embedded into the bone completely, thus avoiding the risk of the irritation to surrounding tissues. (Figure 1b).

The suture spanning technique was achieved by two suture anchors (TWINFIX Ti 3.5 mm with two No. 2 Durabraid Sutures; Smith & Nephew, UK).[22-24] First, the reduction was done manually and secured by one K-wire. Next, the first suture anchor (anchor 1) was inserted obliquely at the 12 o'clock position with a 45° angle in respect to the fracture plane; then, the other one (anchor 2) was inserted beneath the fracture border at the 6 o'clock position. After insertion of the two suture anchors, the four ends of the two strands of anchor 1 all passed the tendon by the free needle for the horizontal mattress suture. Meanwhile, only one end of each strand of anchor 2 passed the tendon and then passed back again. Finally, the sutures of anchor 1 were tied, first to compress the fragment, and then the remaining sutures were tied to secure the fixation (Figure 1a).

Biomechanical testing. In the test, the calcanea were fixed in a custom-made cylinder holder fixed with six screws and cast in polymethyl methacrylate cement. We used ten strands of No. 5 Ti-Cron (Covidien; Medtronic, Ireland) to tube the tendon and fix it to the custom-made tendon binder of the testing machine (Lloyd LRX; AMETEK, USA) (Figure 1c). The test was performed at room temperature. During testing, saline was sprayed to keep the sample wet, as well as to preserve non-tested samples. Before testing, a preload of 25 N was applied

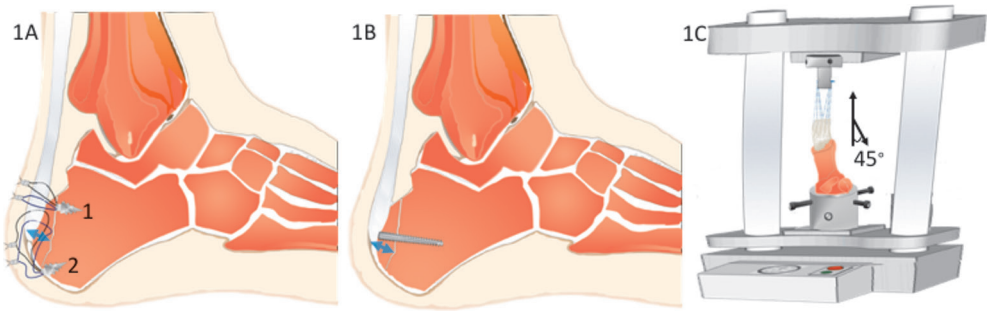

Fig. 1

a) The suture spanning technique with two suture anchors. The blue arrow marks the thickness of the fragment. b) Headless screw fixation for the calcaneal tuberosity fracture. c) The setting of the porcine heel on the material testing machine. To simulate the ankle joint in the postoperative protective condition, the tested angle between the tendon and the long axis of the calcaneal body was set at 45°.

to each sample for 30 seconds for pre-tensioning. Finally, the load-to-failure test was performed to simulate the acute trauma event,[5,25] while the cyclic loading test was used for simulation of postoperative early rehabilitation.[26]

Load-to-failure test. The machine directly pulled the Achilles tendon at a rate of 200 mm/min. The load and elongation were recorded at a frequency of 40 Hz. The load-elongation curve was then plotted for analysis (NEXGEN; Lloyd, UK). The peak failure load (load-to-failure test), stiffness (load-to-failure test), and failure mode were recorded. Peak failure load was defined as the maximal load on the load-elongation curve. Stiffness was the slope of the most linear region of the load-elongation curve. Finally, the failed modes of the two fixation methods were recorded.

Cyclic loading test. In the cyclic loading test, the machine pulled the tendon from 25 N to 500 N for 500 cycles at a speed of 300 mm/min. The number 500 was designated because of the assumption of having 100 cycles of training every weekday during the early staged rehabilitation. The load and elongation were recorded at a frequency of 40 Hz. The difference of the final actuator position between the first and last cycles at a tension of 25 N was defined as the creep. The mean stiffness of the cycles was treated as the mean stiffness of the cyclic loading test. If the samples survived 500 cycles, an additional load-to-failure test would pull the fixation complex until failure, and the maximal load on the load-elongation curve was recorded as the peak failure load (cyclic loading test). If the samples failed the cyclic loading test, the biggest load recorded among the cycles was treated as the peak failure load (cyclic loading test) instead.

Statistical analysis. If R^2 is 0.64 and the effect from the main predictor is 10, three samples per group gave 75% power in the multiple linear regression model assuming α is 0.05. SPSS v26.0 (IBM, USA) was used for the statistical analysis. For all the statistical tests, a p-value < 0.05 is considered statistically significant. One-way analysis of variance (ANOVA) tested the difference in BMD between these six subgroups, while one-sample *t*-test compared the BMD values of the porcine calcanea with the reference value of human calcanea in the literature.[27] One-sample *t*-test also examined the proximity of the measured length, width, and thickness of the fragment to the designated values. This study has two independent variables: one categorical variable and one scale variable. The relationship between these two independent variables and all the outcome measures was examined by correlation analysis (parametric: Pearson correlation test; non-parametric: Spearman correlation test). Point biserial correlation modification was taken when examining the correlation between the outcome measures and fixation methods. If the outcome measure was only correlated to one independent variable, the outcome would be tested by the parametric (independent-samples *t*-test or one-way ANOVA) or nonparametric test (Mann-Whitney U test) according to the normality results examined by the Shapiro-Wilk test. If the outcome measure was correlated to both independent variables, multiple regression analysis was used. The multiple regression analysis took the analysis of covariance (ANCOVA) test when the two independent variables did not have combined effect to the outcome measure. Conversely, when the combined effect existed, moderation analysis was applied. The detailed statistical workflow is shown in Supplementary Figure a.[28]

Results

The length, width, and thickness of the fragment showed no statistical difference from the designated values. The porcine calcaneal BMD was also comparable to the human BMD (p = 0.102, one-sample *t*-test) (Supplementary Table i).[19] The BMD values among the six subgroups were not significantly different (p = 0.120, one-way ANOVA) (Supplementary Figure b).

All the outcome measures passed the normality tests except the mean stiffness in the cyclic loading test (Supplementary Table ii). The mean and 95% confidence intervals (CIs) of all the outcomes are listed in Table I. In the cyclic loading test, all the samples survived the test except the 5 mm samples with headless screw fixation. All the failure modes of the headless screw and suture anchor fixation in the load-to-failure and cyclic loading tests are listed in Table II.

Table I. All outcome measures in the six subgroups.

Outcome measure	Load-to-failure test	
	Suture anchor, mean (95% CI)	**Headless screw, mean (95% CI)**
Peak failure load, N		
5 mm	428.39 (301.47 to 555.32)	267.20 (206.88 to 327.52)
10 mm	358.43 (216.80 to 500.05)	315.75 (282.96 to 348.55)
15 mm	446.58 (361.61 to 531.55)	432.55 (370.30 to 494.80)
Stiffness, N/mm		
5 mm	63.99 (42.88 to 85.10)	73.60 (70.79 to 76.41)
10 mm	52.35 (23.83 to 80.87)	82.67 (68.72 to 96.61)
15 mm	46.23 (35.53 to 56.93)	73.18 (66.66 to 80.36)
	Cyclic loading test	
Peak failure load, N		
5 mm	387.54 (224.49 to 550.59)	224.01 (188.41 to 259.61)
10 mm	354.27 (202.17 to 506.37)	324.30 (288.13 to 360.47)
15 mm	390.76 (356.59 to 424.93)	402.57 (363.82 to 441.33)
Mean stiffness, N/mm		
5 mm	38.17 (24.76 to 51.58)	N/A
10 mm	41.61 (27.17 to 56.06)	42.32 (31.30 to 53.33)
15 mm	35.85 (34.14 to 37.56)	63.43 (46.55 to 80.30)
Creep, mm		
5 mm	10.51 (5.67 to 15.35)	N/A
10 mm	10.10 (6.09 to 14.11)	6.20 (4.87 to 7.54)
15 mm	8.68 (6.84 to 10.53)	3.94 (2.18 to 5.70)

CI, confidence interval; N/A, not applicable.

The correlation evaluation demonstrated that the stiffness in the load-to-failure test and mean stiffness in the cyclic loading test were mainly associated with the fixation methods rather than fragment thickness (Table III). The correlation coefficient (CC) between the stiffness (load-to-failure test) and fixation methods was 0.808 ($p < 0.001$, Pearson correlation test). Similarly, the CC between the mean stiffness (cyclic loading test) and fixation methods was 0.661 ($p = 0.007$, Spearman correlation test). To confirm the effect of fixation methods on the stiffness (load-to-failure test) and mean stiffness (cyclic loading test), independent-samples *t*-test showed a significant difference between the suture anchor and headless screw fixation ($p < 0.001$), while the Mann-Whitney U test showed a significant difference for the mean stiffness (cyclic loading test) ($p = 0.012$) (Figures 2a and 2b). Unlike the stiffness (load-to-failure test) and mean stiffness (cyclic loading test), peak failure load (cyclic loading test) had a significant association with the fragment thickness (CC = 0.541, $p = 0.021$, one-way ANOVA). However, one-way ANOVA could not show significant differences in the peak failure load (cyclic loading test) among the different fragment thickness groups ($p = 0.070$) (Figure 2c).

The peak failure load (load-to-failure test) and creep were significantly correlated with both the fixation method and fragment thickness (Table III); this means that both the fixation methods and fragment thickness affect the value of the peak failure load of load-to-failure test and creep after cyclic loading. Thus, multiple regression analysis is needed to examine the effect of these two variables (Supplementary Figure a). The initial interaction test presented the significant interaction of the fixation methods and fragment thickness, and this interaction affected the peak failure load (load-to-failure test) ($p = 0.018$), but not the creep ($p = 0.246$, both ANCOVA interaction test). The creep then entered the main effect model and demonstrated that the fixation method is the main predictor ($R^2 = 0.83$, $p < 0.001$) (Table IV). In this model, suture anchor fixation tended to have 4.10 mm more creep than headless screw fixation after controlling the thickness (Figure 3b).

Conversely, because of the significant interaction effect of the fixation methods and fragment thickness, the peak failure load (load-to-failure test) could be predicted by fixation methods, fragment thickness, and a combination of the two, as shown in Table IV ($p = 0.001$, $R^2 = 0.67$). In this model, the peak failure load (load-to-failure test) of the headless screw fixation was not comparable to the suture anchors until the achieved thickness was bigger than 15 mm after controlling the fixation methods ($p = 0.980$, ANCOVA). (Figure 3a).

Discussion

The results of this study show that the headless screw fixation for the 15 mm thick simple calcaneal avulsion fracture has comparable peak failure load (load-to-failure test) to the suture anchor fixation as well as less creep after cyclic loading.

To further explain the results, we adopted modified Chapman's formula defining the pullout strength of the conical screw similar to the design of the headless screw.[18]

Modified Chapman's formula:

$$F_{pullout} = S_{shear} \times \pi L D_{0-equ} \times \left(\frac{1}{2} + \frac{1}{\sqrt{3}}\frac{d_{equ}}{p}\right) \times \left(\frac{1-n^2}{1-m^2}\right)^b$$

$$S_{shear} = a\rho^b; m = \frac{D_i - equ}{D_o - equ}; n = \frac{d_p}{D_o - equ}$$

The symbols in the formula are respectively denoted as: $F_{pullout}$: pullout force; S_{shear}: shearing force at the bone-screw plane; L: the screw length within the bone; a,b: the constants associated with bone quality; $D_{i\text{-}equ}$: inner diameter equivalent of the screw; $D_{o\text{-}equ}$: outer diameter equivalent of the screw; d_p: diameter of the predrilling tunnel; p: thread pitch; d_{equ}: thread depth equivalent (Figure 4b).

From the equation, we know that the shearing force (S_{shear}) at the contact plane is related to the bone quality that may vary little in the standardized animal models. The m and n are associated with screw designs and change little along the screw length. This means that the main contributor of peak failure load would be mostly from

Table II. The failure modes of the suture anchor and headless screw fixation in the load-to-failure and cyclic loading tests.

Test	Headless screw			Suture anchor		
	Fracture fragment pullout	Broken screw	Fracture fragment and screw pullout	Broken sutures	Broken eyelet	Anchor pullout
Load-to-failure	6	0	3	9	0	0
Cyclic loading	9	0	0	9	0	0

Table III. The correlation between all the outcome measures and the two independent variables in terms of fixation method and fragment thickness.

Outcome measure	Fx/FT	R^2	Correlation coefficient	p-value
Load-to-failure test				
Peak failure load, N	Fx	0.245	-0.495	0.037*†
	FT	0.261	0.511	0.030*
Stiffness, N/mm	Fx	0.653	0.808	< 0.001*†
	FT	0.269	-0.269	0.280*
Cyclic loading test				
Peak failure load, N	Fx	0.195	-0.441	0.067*†
	FT	0.292	0.541	0.021*
Mean stiffness, N/mm	Fx	0.431	0.661	0.007†‡
	FT	0.177	0.276	0.320‡
Creep, mm	Fx	0.734	-0.857	< 0.001*†
	FT	0.331	-0.575	0.025*

*Pearson correlation test
†Point biserial correlation.
‡Spearman correlation test.
FT, fragment thickness; Fx, fixation method.

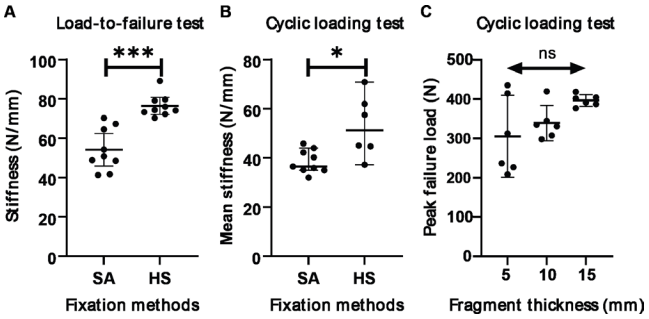

Fig. 2

a) Mean and 95% confidence intervals (CIs) of the stiffness of different fixation methods in the load-to-failure test, and the significant difference between the suture anchors and headless screw fixation. b) The median of the mean stiffness of cyclic loading tests and 95% CIs of the two fixation methods and the significant difference is noted. c) Mean and 95% CIs of the peak failure load of cyclic loading test of different fragment thicknesses, with no significant difference noted among the groups (p = 0.070). ns, p > 0.05, one-way ANOVA; *p < 0.05, Mann-Whitney U test; ***p < 0.001, independent-samples *t*-test. ns, non-significant.

either F_1 or F_2, which are proportional to the embedding screw length (L_1 or L_2) in Figure 4a. We assume that the calcaneal body length is always longer than the avulsed fragment ($L_2 > L_1$), and thus the main contributor of peak failure load (load-to-failure test) would come from F_1. In this case, the failure should pull out the fracture fragment only; however, the pullout of both the fragment and screw happened as the fragment thickness increased to 15 mm. This change of failure modes is due to the use of the screw with a fixed length, so L2 decreases simultaneously as the fragment thickness increases. In real situations, if a longer headless screw is available to keep L2 consistently longer than L1, then the peak failure load (load-to-failure test) of the headless screw should increase along with the increase of the fragment thickness, as in our regression model.

Unlike headless screw fixation, suture anchor fixation failed at sutures and its peak failure load (load-to-failure test) was affected less by the fragment thickness in the regression model. The failure mode of suture anchor fixation implies that its resistance against pulling mainly originates from suture strength. The suture strength of four strands of FiberWire (Arthrex, USA) with three-throw knots is around 250 N[29] but above 400 N with the suture spanning technique, which is the common practice for all kinds of avulsion fractures in the National Taiwan University Hospital. Interestingly, in our regression models the peak failure load (load-to-failure test) of suture anchor fixation is approximated and then exceeded by headless screw fixation when the fragment thickness increases from 10 mm to 15 mm. However, this only applies when the longer headless screw is available to provide long enough L_2.

In the cyclic loading test, all the 5 mm samples of the headless screw fixation failed; this implies that 5 mm is too thin for the headless screw fixation. As long as the fragment thickness increases above 10 mm, headless screw fixation survives the cyclic loading test. Simultaneously, the peak failure load (cyclic loading test) of headless screw fixation is close to the suture anchors. Our findings about peak failure load (load-to-failure test) and peak failure load (cyclic loading test) are different from the literature, where the pullout strength of the suture techniques surpasses the compression screws for the avulsed tibia spine fractures.[30-32] The possible reasons are that these studies use conventional compression screws rather than headless compression screws, thus providing bigger pullout strength.[15] Moreover, the fragment thickness is not taken into account, although it is one of the major factors deciding the pullout strength.

Our study shows that the stiffness (load-to-failure test) and mean stiffness (cyclic loading test) are fixation method-dependent. Stiffness is the force needed to create a certain deformation of a structure. When pulling the fixation complex, the deformation of the headless screw could be from the proximal fragment, titanium

Table IV. The results of multiple regression analysis and regression models for the creep and peak failure load in the load-to-failure test.

Outcome variable	R^2	Intercept	B (fixation)	B (thickness)	B (combined effect of fixation and thickness)	p-value
Creep	0.83	12.13	-4.10*	-0.24	N/A	< 0.001†
Peak failure load (load-to-failure test)	0.67	173.15	219.79	16.53	-14.72	0.001‡

*The reference fixation method was headless screw fixation for the dummy variables (headless screw = 1; suture anchor = 0).
†Analysis of covariance.
‡Moderation analysis.
B, beta coefficient; N/A, not applicable.

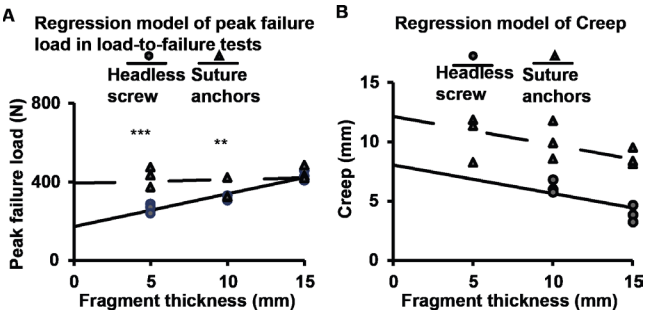

Fig. 3

A) Regression model of the peak failure load of load-to-failure tests. Moderation analysis showed that the peak failure loads of suture anchors and headless screw fixation were significantly different in the 5 mm and 10 mm thick fragment groups. B) Regression model of the creep. By controlling the thickness, the suture anchor fixation tended to have 4.1 mm bigger creep than headless screw with p < 0.001. All the 5 mm thick fragments of headless screw fixation failed the test, and thus no values are shown. **p = 0.006, ***p = 0.001; multiple regression analysis.

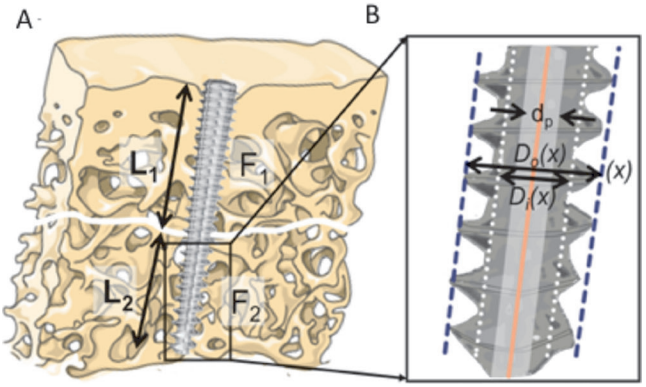

Fig. 4

a) The pullout force of the headless screw fixation originating from F1 or F2. When F1 < F2, the proximal fragment would be pulled out. Conversely, when F1 > F2, the fragment and screw would be pulled out together. b) The pullout force of the screw is associated with the screw design and diameter of the predrilling tunnel (dp). F(1 or 2), the pullout force of the screw; L(1 or 2), the screw length within the bone; X, the specific x position along the screw length; $D_i(X)$, inner diameter of the screw at X position; $D_o(X)$, outer diameter of the screw at X position; dp, diameter of the predrilling tunnel.

screw, and calcaneal body. These three are all hard, solid substances. Unlike headless screw fixation, the deformation of the suture anchor fixation mainly occurs at the sutures or anchor screws. Since sutures are less stiff than anchors, the major deformation may mainly come from the sutures. Therefore, stiffness (load-to-failure test) and mean stiffness (cyclic loading test) are fixation method dependent and smaller in the suture anchor fixation regardless of the fragment thickness.

Since the headless screw fixation complex is stiffer than the suture anchors, there is less deformation after repeated loading than with the suture anchors. This explains why creep is mainly affected by the fixation methods in our regression model. Accordingly, less creep in headless screw fixation is expected, and therefore the patients may be allowed to start earlier rehabilitation.

Our study successfully demonstrated that 4.0 mm diameter headless screw fixation is a possible alternative when fracture fragment thickness is over 15 mm, while suture anchors are a better option for a fracture with a thickness less than 10 mm. Realizing the importance of fragment thickness in avulsion fracture helps to deliver a better value-based treatment, thus fulfilling the patient's needs. However, this is a pilot study and larger clinical studies for simple calcaneal avulsion or similar fractures are needed to validate the findings.

Our study has a number of limitations. As an ex vivo study, the porcine bone morphology and texture of tendons might be not the same as in humans.[33] The calcaneal tuberosity avulsion fracture commonly happens in osteoporotic bones; however, the current study used porcine calcanea with normal bone densities. This may affect the applicability of the study results, although BMD may not have affected the pullout force in previous biomechanical studies.[34,35] Additionally, pulling the fragment unidirectionally at a fixed angle only fulfills the failed mechanism of unidirectional pulling, and does not simulate other failure modes such as shearing or compression. Furthermore, porcine heels are specifically isolated to receive tests while the surrounding bones, muscles, ligaments, and articulation are all removed. These structures may contribute to fixation stability, but are not discussed here.

Both headless screw and suture anchor fixation for the calcaneal avulsion fracture or similar fractures are potentially arthroscopically feasible. However, all the procedures were performed openly. We believe that the open technique could result in more consistent fixation and decrease errors. Meanwhile, this study did not include the common fixation method such as suture anchors combined with compression screws. Despite

these limitations, this study still provides a reference of the optimal thickness to choose headless screw fixation for simple calcaneal avulsion fractures.

In conclusion, this biomechanical study demonstrates that the appropriate thickness for a standard-size headless screw to fix simple calcaneal avulsion fractures is 15 mm in terms of the comparable peak failure load to the suture anchor fixation, with better fixation construct stiffness and less displacement after cyclic loading. Given that the fragment thickness is less than 10 mm, suture anchor fixation seems to be the safer choice.

Supplementary material

Data regarding the standardization of the artificial fracture fragment, as well as the workflow of multiple regression analysis.

References

1. **Schepers T**, **Ginai AZ**, **Van Lieshout EMM**, **Patka P**. Demographics of extra-articular calcaneal fractures: including a review of the literature on treatment and outcome. *Arch Orthop Trauma Surg*. 2008;128(10):1099–1106.
2. **Banerjee R**, **Chao JC**, **Taylor R**, **Siddiqui A**. Management of calcaneal tuberosity fractures. *J Am Acad Orthop Surg*. 2012;20(4):253–258.
3. **Gardner MJ**, **Nork SE**, **Barei DP**, **Kramer PA**, **Sangeorzan BJ**, **Benirschke SK**. Secondary soft tissue compromise in tongue-type calcaneus fractures. *J Orthop Trauma*. 2008;22(7):439–445.
4. **Al-Hourani K**, **Tsang S-T**, **Simpson A**. Osteoporosis: current screening methods, novel techniques, and preoperative assessment of bone mineral density. *Bone Joint Res*. 2021;10(12):840–843.
5. **Feng X**, **Qi W**, **Fang CX**, **Lu WW**, **Leung FKL**, **Chen B**. Can barb thread design improve the pullout strength of bone screws? *Bone Joint Res*. 2021;10(2):105–112.
6. **Dickenson EJ**, **Parsons N**, **Griffin DR**. Open reduction and internal fixation versus nonoperative treatment for closed, displaced, intra-articular fractures of the calcaneus: long-term follow-up from the HeFT randomized controlled trial. *Bone Joint J*. 2021;103-B(6):1040–1046.
7. **Lui TH**. Fixation of tendo Achilles avulsion fracture. *Foot Ankle Surg*. 2009;15(2):58–61.
8. **Banerjee R**, **Chao J**, **Sadeghi C**, **Taylor R**, **Nickisch F**. Fractures of the calcaneal tuberosity treated with suture fixation through bone tunnels. *J Orthop Trauma*. 2011;25(11):685–690.
9. **Squires B**, **Allen PE**, **Livingstone J**, **Atkins RM**. Fractures of the tuberosity of the calcaneus. *J Bone Joint Surg Br*. 2001;83-B(1):55–61.
10. **Beavis RC**, **Rourke K**, **Court-Brown C**. Avulsion fracture of the calcaneal tuberosity: a case report and literature review. *Foot Ankle Int*. 2008;29(8):863–866.
11. **Khazen GE**, **Wilson AN**, **Ashfaq S**, **Parks BG**, **Schon LC**. Fixation of calcaneal avulsion fractures using screws with and without suture anchors: a biomechanical investigation. *Foot Ankle Int*. 2007;28(11):1183–1186.
12. **Wang Q**, **Li X**, **Sun Y**, **Yan L**, **Xiong C**, **Wang J**. Comparison of the outcomes of two operational methods used for the fixation of calcaneal fracture. *Cell Biochem Biophys*. 2015;72(1):191–196.
13. **Lui TH**. Avulsion fracture of the posterosuperior tuberosity of the calcaneus managed with lag screw fixation. *Foot Ankle Surg*. 2018;24(1):45–48.
14. **Mitchell PM**, **O'Neill DE**, **Branch E**, **Mir HR**, **Sanders RW**, **Collinge CA**. Calcaneal avulsion fractures: A multicenter analysis of soft-tissue compromise and early fixation failure. *J Orthop Trauma*. 2019;33(11):e422–e426.
15. **Wheeler DL**, **McLoughlin SW**. Biomechanical assessment of compression screws. *Clin Orthop Relat Res*. 1998;350:237–245.
16. **Sugathan HK**, **Kilpatrick M**, **Joyce TJ**, **Harrison JWK**. A biomechanical study on variation of compressive force along the Acutrak 2 screw. *Injury*. 2012;43(2):205–208.
17. **Beadel GP**, **Ferreira L**, **Johnson JA**, **King GJW**. Interfragmentary compression across a simulated scaphoid fracture--analysis of 3 screws. *J Hand Surg Am*. 2004;29(2):273–278.
18. **Tsai W-C**, **Chen P-Q**, **Lu T-W**, **Wu S-S**, **Shih K-S**, **Lin S-C**. Comparison and prediction of pullout strength of conical and cylindrical pedicle screws within synthetic bone. *BMC Musculoskelet Disord*. 2009;10:44.
19. **Robertson G**, **Wallace R**, **Simpson A**, **Dawson SP**. Preoperative measures of bone mineral density from digital wrist radiographs. *Bone Joint Res*. 2021;10(12):830–839.
20. **Hildebrand TOR**, **Rüegsegger P**. Quantification of bone microarchitecture with the structure model index. *Comput Methods Biomech Biomed Engin*. 1997;1(1):15–23.
21. **Schmidutz F**, **Schopf C**, **Yan SG**, **Ahrend M-D**, **Ihle C**, **Sprecher C**. Cortical bone thickness of the distal radius predicts the local bone mineral density. *Bone Joint Res*. 2021;10(12):820–829.
22. **Ji J-H**, **Kim W-Y**, **Ra K-H**. Arthroscopic double-row suture anchor fixation of minimally displaced greater tuberosity fractures. *Arthroscopy*. 2007;23(10):1133.
23. **Kim K-C**, **Rhee K-J**, **Shin H-D**, **Kim Y-M**. Arthroscopic fixation for displaced greater tuberosity fracture using the suture-bridge technique. *Arthroscopy*. 2008;24(1):120.
24. **Cho BK**, **Park JK**, **Choi SM**. Reattachment using the suture bridge augmentation for Achilles tendon avulsion fracture with osteoporotic bony fragment. *Foot*. 2017;31:35–39.
25. **Beynnon BD**, **Amis AA**. In vitro testing protocols for the cruciate ligaments and ligament reconstructions. *Knee Surg Sports Traumatol Arthrosc*. 1998;6 Suppl 1:S70–6.
26. **Shelburne KB**, **Pandy MG**, **Anderson FC**, **Torry MR**. Pattern of anterior cruciate ligament force in normal walking. *J Biomech*. 2004;37(6):797–805.
27. **Mittra E**, **Rubin C**, **Gruber B**, **Qin Y-X**. Evaluation of trabecular mechanical and microstructural properties in human calcaneal bone of advanced age using mechanical testing, microCT, and DXA. *J Biomech*. 2008;41(2):368–375.
28. **Hayes AF**. *Introduction to Mediation, Moderation, and Conditional Process Analysis: A Regression-Based Approach*. Fourth ed. New York, New York: The Guilford Press, 2018.
29. **Komatsu F**, **Mori R**, **Uchio Y**. Optimum surgical suture material and methods to obtain high tensile strength at knots: problems of conventional knots and the reinforcement effect of adhesive agent. *J Orthop Sci*. 2006;11(1):70–74.
30. **Li J**, **Yu Y**, **Liu C**, **Su X**, **Liao W**, **Li Z**. Arthroscopic fixation of tibial eminence fractures: A biomechanical comparative study of screw, suture, and suture anchor. *Arthroscopy*. 2018;34(5):1608–1616.
31. **Anderson CN**, **Nyman JS**, **McCullough KA**, **et al**. Biomechanical evaluation of physeal-sparing fixation methods in tibial eminence fractures. *Am J Sports Med*. 2013;41(7):1586–1594.
32. **Bong MR**, **Romero A**, **Kubiak E**, **et al**. Suture versus screw fixation of displaced tibial eminence fractures: a biomechanical comparison. *Arthroscopy*. 2005;21(10):1172–1176.
33. **Liebschner MAK**. Biomechanical considerations of animal models used in tissue engineering of bone. *Biomaterials*. 2004;25(9):1697–1714.
34. **Pearce AI**, **Richards RG**, **Milz S**, **Schneider E**, **Pearce SG**. Animal models for implant biomaterial research in bone: a review. *Eur Cell Mater*. 2007;13:1–10.
35. **Lenz M**, **Gueorguiev B**, **Garces JBG**, **et al**. Axial and shear pullout forces of composite, porcine and human metatarsal and cuboid bones. *J Orthop Translat*. 2018;14:67–73.

Author information:

- C. Wang, MD, PhD researcher, Material Department, Imperial College London, London, UK.
- S-J. Liu, PhD, Professor, Department of Mechanical Engineering, Chang Gung University, Taoyuan City, Taiwan.
- C-H. Chang, MD, PhD, Orthopaedic surgeon consultant, Orthopaedic Department, National Taiwan University Hospital, Taipei City, Taiwan.

Author contributions:

- C. Wang: Conceptualization, Data curation, Formal analysis, Investigation, Methodology, Project administration, Software, Validation, Visualization, Writing – original draft, Writing – review & editing.
- S-J. Liu: Data curation, Formal analysis, Methodology, Validation, Writing – review & editing.
- C-H. Chang: Conceptualization, Data curation, Methodology, Supervision, Resources, Validation, Writing – review & editing.

Funding statement:

- The authors received no financial or material support for the research, authorship, and/or publication of this article.

ICMJE COI statement:

- C-H. Chang reports a personal grant (Hospital Research Grant) from National Taiwan University Hospital, related to this study. Each author certifies that he has no commercial associations (e.g., consultancies, stock ownership, equity interest, patent/licensing arrangements, etc.) that might pose a conflict of interest in connection with the submitted article. Some of the results had been presented in the Free Paper presentation at the 39th SICOT Orthopedic World Congress. The title was "A biomechanical study on the pullout strength of suture anchors versus headless screws in avulsion fractures of different thickness".

Data sharing:
- The data that support the findings for this study are available to other researchers from the corresponding author upon reasonable request.

Acknowledgements:
- C. Wang and C-H. Chang acknowledge the financial support from National Taiwan University Hospital (104-N2834).

Open access funding:
- The authors report that the open access funding for their manuscript was self-funded.